Available online at www.sciencedirect.com
SCIENCE DIRECT®
Journal of Theoretical Biology 226 (2004) 143–157
Journal of Theoretical Biology
www.elsevier.com/locate/jtbi

Growth of mixed cultures on mixtures of substitutable substrates: the operating diagram for a structured model

Gregory T. Reeves[a], Atul Narang[b,*], Sergei S. Pilyugin[c]

[a] Department of Chemical Engineering, Princeton University, Princeton, NJ 08544, USA
[b] Department of Chemical Engineering, College of Engineering, University of Florida, Gainesville, FL 32611, USA
[c] Department of Mathematics, University of Florida, Gainesville, FL 32611-8105, USA

Received 22 February 2003; received in revised form 13 July 2003; accepted 15 July 2003

Abstract

The growth of mixed microbial cultures on mixtures of substrates is a problem of fundamental biological interest. In the last two decades, several unstructured models of mixed-substrate growth have been studied. It is well known, however, that the growth patterns in mixed-substrate environments are dictated by the enzymes that catalyse the transport of substrates into the cell. We have shown previously that a model taking due account of transport enzymes captures and explains all the observed patterns of growth of a single species on two substitutable substrates (J. Theor. Biol. 190 (1998) 241). Here, we extend the model to study the steady states of growth of two species on two substitutable substrates. The model is analysed to determine the conditions for existence and stability of the various steady states. Simulations are performed to determine the flow rates and feed concentrations at which both species coexist. We show that if the interaction between the two species is purely competitive, then at any given flow rate, coexistence is possible only if the ratio of the two feed concentrations lies within a certain interval; excessive supply of either one of the two substrates leads to annihilation of one of the species. This result simplifies the construction of the operating diagram for purely competing species. This is because the two-dimensional surface that bounds the flow rates and feed concentrations at which both species coexist has a particularly simple geometry: It is completely determined by only two coordinates, the flow rate and the ratio of the two feed concentrations. We also study commensalistic interactions between the two species by assuming that one of the species excretes a product that can support the growth of the other species. We show that such interactions enhance the coexistence region.

Keywords: Microbial growth; Mathematical model; Mixed cultures; Mixed substrate; Substitutable substrates; Coexistence

1. Introduction

The growth of mixed cultures on mixtures of substrates is a phenomenon of considerable practical and theoretical interest. A fundamental understanding of this problem has repercussions for

- *Food processing*: Cheese is manufactured by mixtures of *Streptococci* and *Lactobacilli*, and yogurt is the product of *Lactobacillus bulgaricus* and *Streptococcus thermophilus*. The production of sauerkraut, beer, wine, and vinegar also depends on mixed-culture systems (Harrison and Wren, 1976).
- *Production of ethanol from renewable resources*: The feedstock for production of fuel-grade ethanol from plants consists of two streams derived from the cellulosic and the hemicellulosic fractions of lignocellulose. The cellulosic stream consists of hexoses; the hemicellulosic stream contains a mixture of pentoses and hexoses. In the current process, each of these streams is fermented separately by distinct recombinant strains. To make this process economically viable, it would be desirable to carry out both fermentations in a single reactor (Ingram et al., 1999).
- *Bioremediation*: Xenobiotic contaminants degrade faster if they are attacked by microbial consortia, rather than pure species.

The problem also has profound implications for microbial ecology. Early studies were concerned with the growth of multiple species on a single

*Corresponding author. Tel.: +1-352-392-0028; fax: +1-352-392-9513.
E-mail address: narang@che.ufl.edu (A. Narang).

0022-5193/$ - see front matter © 2003 Elsevier Ltd. All rights reserved.
doi:10.1016/S0022-5193(03)00280-7

growth-limiting substrate that is being fed at a constant rate into a well-stirred chemostat. It was shown both theoretically and experimentally that under these conditions, no more than one of the species survives, regardless of the dilution rate and the feed concentration of the growth-limiting substrate (Aris and Humphrey, 1977; Hansen and Hubbell, 1980; Powell, 1958). This result is in sharp contrast to what is observed in Nature. In large bodies of water, many phytoplankton species coexist, an observation referred to as the "paradox of the plankton" (Hutchinson, 1961). To resolve this paradox, the basic assumptions of the early studies have been questioned (Fredrickson and Stephanopoulos, 1981). It has been argued that in Nature

- the supply of nutrients is not constant;
- the nutrients are not homogeneously distributed;
- multiple growth-limiting substrates are present in the environment.

Thus, the problem of mixed-culture growth on mixtures of substrates has attracted considerable interest as one possible resolution of the paradox of the plankton. This initial interest culminated in two seminal papers which recognized that in the presence of multiple growth-limiting substrates, it is important to specify the nutritional requirements satisfied by the substrates (León and Tumpson, 1975; Tilman, 1977). Thus, two growth-limiting substrates are *substitutable* if they satisfy identical nutritional requirements, so that growth persists in the absence of either one of the substrates. The two substrates are *complementary* if they satisfy distinct nutritional requirements, so that growth is impossible in the absence of either one of the substrates. For example, during so-called heterotrophic growth of microbes, glucose and galactose would be considered substitutable since both function as carbon and energy sources, but glucose and ammonia would be complementary since glucose is a carbon source, whereas ammonia is a nitrogen source. In both studies, unstructured models of mixed-culture growth on substitutable and complementary mixtures of substrates were formulated, and necessary conditions for coexistence of the species were derived. But the use of unstructured models ignores the fact that uptake of substrates is regulated by the activity and level of the transport enzymes. In mixtures of substitutable substrates, this regulation often leads to preferential utilization of only one of the substrates (Egli 1995; Harder and Dijkhuizen, 1976; 1982). It seems desirable then to study the problem of mixed-culture growth on mixtures of substrates with the help of a structured model that takes due account of the transport enzymes and their regulation. In earlier work, we formulated such a model for the growth of a single species on mixtures of substitutable substrates, and showed that it captures and explains all the experimental data in the literature (Narang et al., 1997; Narang, 1998a,b). Here, we extend this model to study the growth of two species on a mixture of two substitutable substrates.

Despite the importance of the problem, review articles show that the experimental data are sparse (Fredrickson, 1977; Gottschal, 1986, 1993). This reflects the difficulty of measuring the population densities of multiple species. In the past, this was done by exploiting morphological differences between the species, or by selective plating techniques in which inhibitors are added to block the growth of all but one of the species. These methods are tedious and prone to error. Recent developments in flow cytometry and 16S RNA-based probes permit quick and accurate measurements of multiple population densities (Porter and Pickup, 2000). These technological advances are likely to foster rapid growth of the experimental literature on mixed cultures (for recent applications, see Muller et al., 2000; Rogers et al., 2000). The goal of this paper is to submit conclusions derived from a structured model that can be subjected to the test of these experiments. We shall be concerned, in particular, with the following questions

1. What are the flow rates and feed concentrations of the two substitutable substrates at which both species coexist?
2. How is their coexistence affected if one of the species excretes a product that influences the growth of the other species?

The first question is the crux of the ecological problem referred to above. The second question is important because pure competition between species is an idealization that is difficult to realize in practice. Most microbial species excrete metabolic products that can stimulate or inhibit the specific growth rate of the other species; this results in the establishment of *commensalistic* or *amensalistic*, rather than competitive, interactions (Fredrickson and Tsuchiya, 1977). It is, therefore, of practical interest to assess the effect of excretion on the phenomenon of coexistence.

The paper is organized as follows. In Section 2, we extend our earlier model of mixed-substrate growth to mixed cultures. In Section 3, we compute the operating diagram delineating the region of the parameter space in which coexistence is feasible (Pavlou and Fredrickson, 1989). This is done for two types of inter-specific interactions—pure competition and commensalism. Finally, the conclusions are summarized in Section 4. The key results are as follows:

1. If the interaction between the two species is purely competitive, then:
   (a) At any given flow rate, coexistence is possible only if the ratio of the two feed concentrations lies within a certain interval. Excessive supply

of either one of the two substrates results in extinction of one of the species.

(b) The operating diagram delineating the flow rate and feed concentrations at which the two species coexist has a particularly simple geometry.

2. If, however, one of the species excretes a product that can support the growth of the other species, the coexistence region is significantly enhanced.

2. Model

The kinetic scheme of our model is shown in Fig. 1. As a notational convention for the rest of the paper, the index i will denote the species number, and the index j will denote the substrate number. Thus, C_i denotes the ith species, S_j denotes the jth substrate, E_{ij} denotes the "lumped" system of inducible enzymes catalysing the uptake and peripheral catabolism of S_j by C_i, X_{ij} denotes the inducer for E_{ij}, and C_i^- denotes all intracellular constituents in the ith species, except E_{ij} and X_{ij}. The concentrations of these entities are denoted by the lower-case letters c_i, s_j, e_{ij}, x_{ij}, and c_i^-. Here, c_i and s_j are based on the volume of the chemostat, and expressed in the units gdw/l and g/l, respectively; the remaining variables, x_{ij}, e_{ij} and c_i^- are based on the dry weight of the biomass, and expressed in the units g/gdw. The yield, denoted Y_{ij}, is the fraction of X_{ij} that is converted into C_i^-; the remainder, $1-Y_{ij}$, is expelled into the environment as carbon dioxide or partially oxidized excretory products.

The following assumptions are made regarding the kinetics of the various processes:

1. The specific uptake rate of the jth substrate by the ith species, denoted r_{ij}^s, satisfies the kinetic law
$$r_{ij}^s \equiv V_{ij}^s e_{ij} \frac{s_j}{K_{ij}^s + s_j}.$$

2. The specific rate of breakdown of X_{ij} into energy and C_i^-, denoted r_{ij}^x, is given by
$$r_{ij}^x \equiv k_{ij}^x x_{ij}.$$

3. The yield, Y_{ij}, is a fixed "stoichiometric" coefficient. That is, the rates of non-biosynthetic processes, such as overflow metabolism, energy spillage, and maintenance, are proportional to the biosynthetic rate.

4. The specific rate of *inducible* enzyme synthesis, denoted r_{ij}^e, is hyperbolic with respect to x_{ij}:
$$r_{ij}^e \equiv V_{ij}^e \frac{x_{ij}}{K_{ij}^e + x_{ij}}.$$

5. The specific rate of *constitutive* enzyme synthesis, denoted r_{ij}^*, is constant:
$$r_{ij}^* \equiv k_{ij}^*,$$
where k_{ij}^* denotes the zeroth-order rate constant.

6. The specific rate of enzyme degradation, denoted r_{ij}^d, follows first-order kinetics
$$r_{ij}^d \equiv k_{ij}^d e_{ij}.$$

A mass balance on the state variables yields

$$\frac{ds_j}{dt} = D(s_j^f - s_j) - r_{1j}^s c_1 - r_{2j}^s c_2, \tag{1}$$

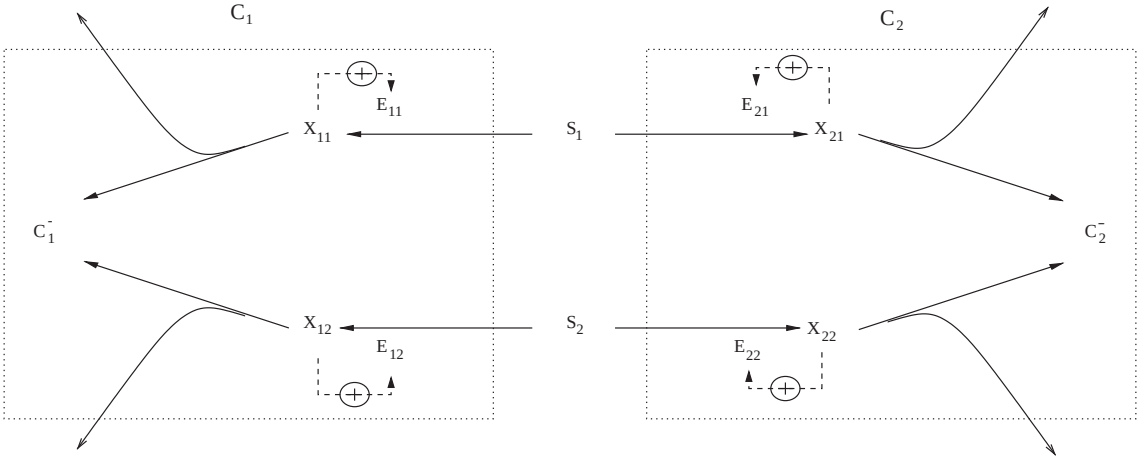

Fig. 1. Kinetic scheme of the model. Here, C_1 and C_2 denote the two species competing for the substitutable substrates, S_1 and S_2, E_{ij} denotes the transport enzyme of the ith species for the jth substrate, X_{ij} denotes the inducer for E_{ij}, and C_i^- denotes all intracellular components of C_i, except E_{ij} and X_{ij}.

$$\frac{dx_{ij}}{dt} = r^s_{ij} - r^x_{ij} - \left(D + \frac{1}{c_i}\frac{dc_i}{dt}\right)x_{ij}, \quad (2)$$

$$\frac{de_{ij}}{dt} = r^e_{ij} + r^*_{ij} - r^d_{ij} - \left(D + \frac{1}{c_i}\frac{dc_i}{dt}\right)e_{ij}, \quad (3)$$

$$\frac{dc^-_i}{dt} = \sum_{j=1}^{2}(Y_{ij}r^x_{ij} + r^d_{ij} - r^e_{ij} - r^*_{ij}) - \left(D + \frac{1}{c_i}\frac{dc_i}{dt}\right)c^-_i, \quad (4)$$

where s^f_j denotes the concentration of S_j in the feed, and D denotes the dilution rate. The last terms in Eqs. (2)–(4) represent the loss of X_{ij}, E_{ij}, and C^-_i, respectively, due to flow out of the chemostat and dilution by growth. It is shown in Appendix A that for all but a negligibly small initial time interval, Eqs. (2)–(4) are well approximated by the equations

$$\frac{ds_j}{dt} = D(s^f_j - s_j) - r^s_{1j}c_1 - r^s_{2j}c_2, \quad (5)$$

$$\frac{de_{ij}}{dt} = V^e_{ij}\frac{e_{ij}\sigma_{ij}}{\bar{K}^e_{ij} + e_{ij}\sigma_{ij}} + k^*_{ij} - k^d_{ij}e_{ij} - r^g_i e_{ij}, \quad (6)$$

$$\frac{dc_i}{dt} = (r^g_i - D)c_i, \quad (7)$$

where

$$\bar{K}^e_{ij} \equiv \frac{K^e_{ij}k^x_{ij}}{V^s_{ij}}, \quad \sigma_{ij} \equiv \frac{s_j}{K^s_{ij} + s_j}$$

and r^g_i, the specific growth rate of the ith species, is given by

$$r^g_i \equiv Y_{i1}r^s_{i1} + Y_{i2}r^s_{i2} = Y_{i1}V^s_{i1}e_{i1}\sigma_{i1} + Y_{i2}V^s_{i2}e_{i2}\sigma_{i2}.$$

This is an eight-dimensional system with three control parameters of interest, namely, the dilution rate, D, and the two feed concentrations, s^f_1 and s^f_2.

Evidently, the model admits four types of steady states, which are as follows:

1. The trivial steady state, characterized by $c_1 = c_2 = 0$, denoted by ϕ_{00}.
2. The semitrivial steady states, where exactly one cell density is nonzero:
   (a) ϕ_{10} characterized by $c_1 > 0, c_2 = 0$,
   (b) ϕ_{01} characterized by $c_1 = 0, c_2 > 0$.
3. And the nontrivial, or coexistence, steady state with both $c_1 > 0, c_2 > 0$, denoted by ϕ_{11}.

For a more detailed anaylsis of the properties of the four types of steady states, see Appendixes A–D. Hereafter, we shall be concerned with the construction of the operating diagram that delineates the parameter space in which the two species can coexist.

3. Simulations

The simulations were done using *Mathematica* (Wolfram, 1999) and CONTENT (Kuznetsov, 1998). The parameter values used in the simulations are shown in Table 1. Appendix C shows the rationale for order-of-magnitude estimates of the parameters. The parameter values were then adjusted to ensure that C_1 and C_2 have *opposite* substrate preferences. Specifically, the parameter values for C_1 were chosen so that S_1 is the preferred substrate for C_1; that is, s_1 approaches s^f_1 at a rate slower than the rate at which s_2 approaches s^f_2 (Fig. 2a). This occurs because synthesis of E_{12}, the enzyme that catalyses the transport of S_2, cannot be sustained at sufficiently large dilution rates (see (Narang, 1998a) for more detail). Likewise, the parameter values for C_2 were chosen such that S_2 is the preferred substrate for C_2 (Fig. 2b). To make matters concrete, one can imagine C_1 as a coliform, say, *Escherichia coli*, that prefers a sugar (S_1) over an organic acid (S_2), and C_2 as a pseudomonad, say, *Pseudomonas aeruginosa*, that prefers the organic acid over the sugar (Chian and Mateles, 1968; Kim and Dhurjati, 1986).

3.1. Existence of competition

Our first simulation allows both C_1 and C_2 to grow in a chemostat fed with relatively high concentrations of S_1 and S_2. Fig. 3 shows the steady-state cell densities of C_1 and C_2 as a function of D at fixed feed concentrations, $s^f_1 = 1$ g/l and $s^f_2 = 2$ g/l. In Fig. 3a, one of the steady states corresponds to the semi-trivial steady state, ϕ_{10},

Table 1
Parameter values used in the simulations

$V^s_{11} = 1000$	$V^s_{12} = 1000$	$V^s_{21} = 1000$	$V^s_{22} = 1000$	$V^s_{23} = 1000$	g/g h
$K^s_{11} = 0.01$	$K^s_{12} = 0.01$	$K^s_{21} = 0.01$	$K^s_{22} = 0.01$	$K^s_{23} = 0.01$	g/l
$V^e_{11} = 0.0025$	$V^e_{12} = 0.0020$	$V^e_{21} = 0.0006$	$V^e_{22} = 0.0036$	$V^e_{23} = 0.0015$	g/gdw h
$\bar{K}^e_{11} = 0.0017$	$\bar{K}^e_{12} = 0.0032$	$\bar{K}^e_{21} = 0.0013$	$\bar{K}^e_{22} = 0.0030$	$\bar{K}^e_{23} = 0.0020$	g/gdw
$k^d_{11} = 0.01$	$k^d_{12} = 0.01$	$k^d_{21} = 0.01$	$k^d_{22} = 0.01$	$k^d_{23} = 0.01$	1/h
$k^*_{11} = 10^{-2}\ V^e_{11}$	$k^*_{12} = 10^{-2}\ V^e_{12}$	$k^*_{21} = 10^{-2}\ V^e_{21}$	$k^*_{22} = 10^{-2}\ V^e_{22}$	$k^*_{23} = 10^{-2}\ V^e_{22}$	g/gdw h
$Y_{11} = 0.41$	$Y_{12} = 0.24$	$Y_{21} = 0.35$	$Y_{22} = 0.20$	$Y_{23} = 0.17$	g/g

The orders of magnitude of the parameters were estimated as shown in Appendix C. The values of V^e_{ij} and $\bar{K}^e_{ij}$ were then adjusted so that the single-substrate maximum specific growth rates of C_1 on S_1 and S_2 were 0.73 and 0.41 1/h, respectively, and the single-substrate maximum specific growth rates of C_2 on S_1, S_2, and S_3 were 0.30, 0.60, and 0.36 1/h, respectively. Here, S_3 denotes the product excreted by C_1 and consumed by C_2 (see Section 3.4 for details).

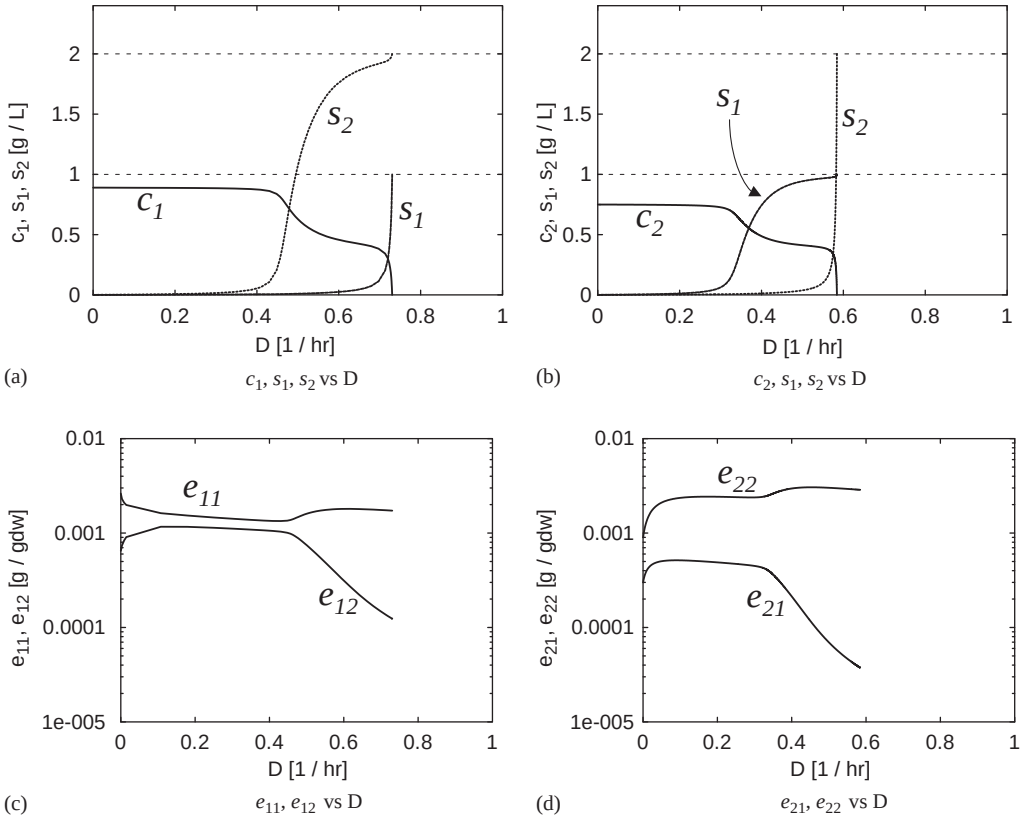

Fig. 2. Steady states of single-species growth on S_1 and S_2. The figures on the left correspond to growth of C_1 on S_1 and S_2. Here, C_1 prefers S_1 in the sense that S_1 approaches s_1^f at a slower rate than S_2 approaches s_2^f. The figures on the right correspond to growth of C_2 on S_1 and S_2 and show that C_2 prefers S_2.

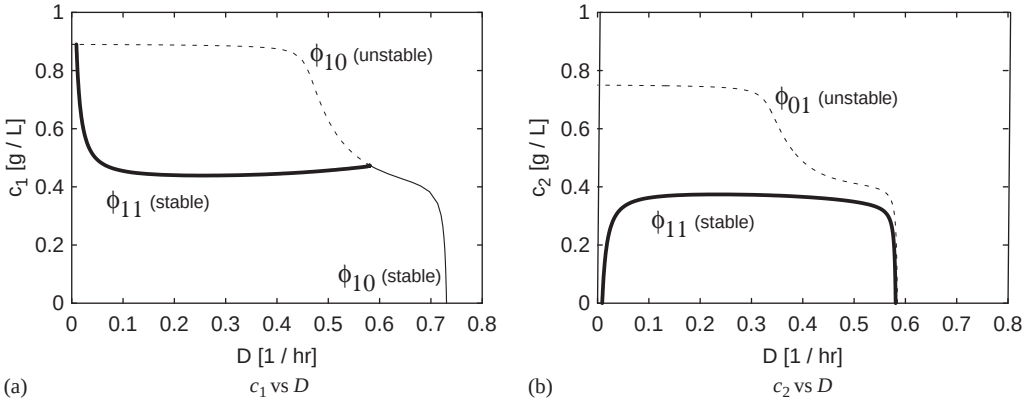

Fig. 3. Variation of c_1 and c_2 with respect to D at feed concentrations, $s_1^f = 1$ g/l and $s_2^f = 2$ g/l. Note that c_2 vanishes at large and at small dilution rates. The washout at the large dilution rate occurs because the flow rate exceeds the maximum specific growth rate of C_2. The washout at the low dilution rate occurs due to competition between the two species.

that would occur if C_1 were the only species in the chemostat; the other is the non-trivial steady state, ϕ_{11}, corresponding to the coexistence of both species. Likewise, in Fig. 3b, one of the steady states corresponds to the semi-trivial steady-state ϕ_{01}, that would occur if C_2 were the only species in the chemostat; it is unstable at all dilution rates. The other steady state is the non-trivial steady state, ϕ_{11}. We see that two striking features emerge when the chemostat is seeded with C_1 and C_2, both of which are the outcome of competition between the two species:

1. Whenever the two species coexist, their steady-state cell densities are lower than the cell densities sustained in the absence of the other species. This suggests the existence of competition.

2. The intensity of competition depends on the dilution rate:
   (a) At large dilution rates, there is competition, but the two species coexist.
   (b) At low dilution rates, the competition becomes so intense that C_2 is outcompeted.

We denote the low dilution rate at which C_2 vanishes by D_2^c, the *competition* dilution rate for C_2. It should be distinguished from the high dilution rate, D_2^w, at which C_2 washes out because the specific growth rate of C_2 is not large enough to withstand the large flow of C_2 out of the reactor.

3.2. Effect of feed concentrations on the competition

We showed above that the introduction of both C_1 and C_2 in the chemostat results in competition between the two species; furthermore, at low dilution rates, the competition becomes particularly intense, and C_2 is rendered extinct. Now, intuition suggests that if we reduce the feed concentration of S_2, the preferred substrate for C_2, its ability to compete would be undermined even further. It then seems plausible that the lower the value of s_2^f, the higher the dilution rate at which C_2 would be outcompeted by C_1. This intuition is borne out by the simulations. Fig. 4 shows c_2 as a function of D when s_1^f is fixed at 1 g/l, but s_2^f is reduced from 2 g/l to various lower concentrations. It can be seen that the smaller the value of s_2^f, the larger the dilution rate at which C_2 is outcompeted by C_1. Indeed, the interval of coexistence shrinks progressively until at a sufficiently small value of s_2^f, it reduces to a point. At even smaller values of s_2^f, C_2's ability to compete has been undermined so severely that it is outcompeted by C_1, and hence, cannot coexist with C_1, at *any* dilution rate. These results are consistent with what we know about the limiting case obtained if s_1^f is held fixed and s_2^f is reduced progressively to zero—we obtain, in effect, a system in which the two species compete for only one substrate. It has been shown that in such single-substrate systems, no more than one species can survive (Hansen and Hubbell, 1980; Powell, 1958).

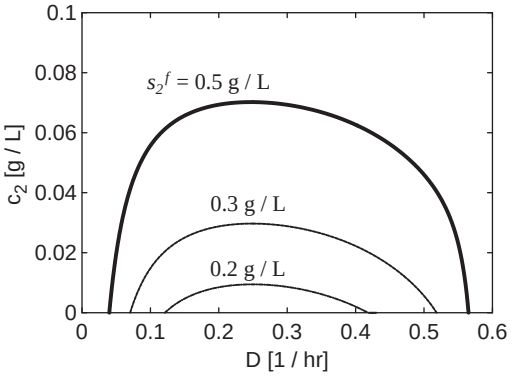

Fig. 4. Variation of c_2 with respect to D at feed concentrations $s_1^f = 1$ g/l and $s_2^f = 0.5, 0.3, 0.2$ g/l. The range of dilution rates at which C_2 exists becomes smaller as s_2^f decreases. This is because C_2 prefers S_2; hence, depriving C_2 of its preferred substrate compromises its ability to compete with C_1.

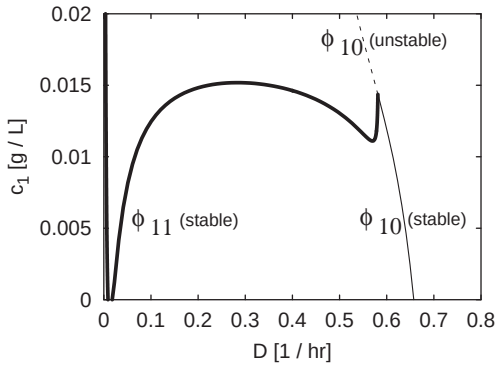

Fig. 5. Variation of c_1 with respect to D at feed concentrations $s_1^f = 0.05$ g/l and $s_2^f = 2$ g/l. This figure illustrates the same principle shown in Fig. 4, the only difference being that we have reduced the feed concentration of S_1, the substrate preferred by C_1. Thus, it is C_1 rather than C_2 that is outcompeted at small dilution rates.

We have established that C_2's ability to compete can be drastically undermined by reducing the supply of S_2, its preferred substrate. This suggests that C_1 is not absolutely superior to C_2. By depriving C_1 of its preferred substrate, S_1, it should be possible to compromise its ability to compete to such an extent that it is outcompeted by C_2. This is also borne out by the simulations. Fig. 5 shows that if s_2^f is held fixed at 2 g/l, but s_1^f is reduced to 0.05 g/l, it is C_1 that vanishes at a low dilution rate. Interestingly, C_1 is resurrected if the dilution rate is reduced even further, a point to which we shall return later. Here, it suffices to note that the ability of C_1 to compete can be significantly compromised by reducing the feed concentration of its preferred substrate, S_1.

3.3. The operating diagram

Our goal is to determine the subset of the $s_1^f s_2^f D$-space in which C_1 and C_2 coexist. To this end, we begin by determining the two-dimensional surfaces that separate the region in which C_1 and C_2 can coexist from the region in which only one of the species persists. We shall then show that the surfaces have a very special geometry which simplifies the description of the $s_1^f s_2^f D$-space in which C_1 and C_2 coexist. It will turn out that this three-dimensional subset can be characterized by two suitably defined curves on a plane.

3.3.1. The boundary between extinction of C_2 and coexistence

To find the surface in the $s_1^f s_2^f D$-space that separates the region in which both species coexist from the region

in which C_2 cannot survive, we seek the surface satisfying the conditions

$$r_1^g = D, \quad r_2^g = D, \quad c_2 = 0.$$

This surface was computed by rewriting the governing steady-state equations to reflect the above conditions as follows:

$$0 = \frac{s_1^f - s_1}{s_2^f - s_2} - \frac{r_{11}^s}{r_{12}^s}, \tag{8}$$

$$0 = r_{ij}^e + k_{ij}^* - (D + k_{ij}^d)e_{ij}, \tag{9}$$

$$0 = r_i^g - D. \tag{10}$$

In the above equations, Eq. (8) is a combination of $(5,\ j = 1, 2)$ with $c_2 = 0$. Eq. (9) is the steady-state version of Eq. (6), and Eq. (10) is Eq. (7) rewritten without the cell densities. Since two equations were combined into one, we lost one degree of freedom. However, since we also eliminated the cell densities, the coordinate variables changed from s_j, e_{ij}, c_i to s_j, e_{ij}. This means there is an extra constraint; now the equations fix D as well. Once an initial point on this surface was obtained, the surface was continued along contours of constant s_1^f (see Fig. 6a). The surface is dual-valued for most feed concentrations because there are typically

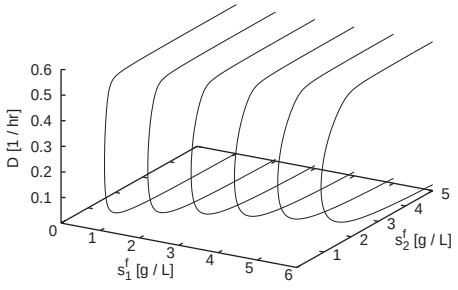

(a) Constant s_1^f contours

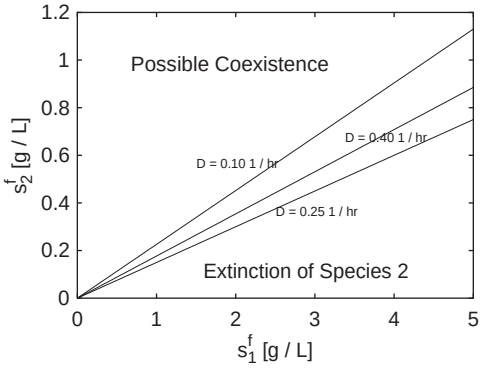

(b) Projection of constant D contours onto the $s_1^f s_2^f$-plane.

Fig. 6. Contours of the surface in the $s_1^f s_2^f D$-space separating the coexistence region from the region in which C_2 is outcompeted. (a) "Inside" the surface, both species coexist; outside it, C_2 vanishes. (b) At each dilution rate, C_2 cannot exist at feed concentrations lying below the line corresponding to that dilution rate.

two dilution rates at which c_2 becomes zero—the low competition dilution rate, D_2^c, and the high washout critical dilution rate, D_2^w. Inside the surface, both species coexist; outside the surface, C_2 cannot exist.

In Fig. 4, it was shown that if s_1^f is held fixed, but s_2^f is progressively decreased, the competition dilution rate, D_2^c, and the washout dilution rate, D_2^w, become closer and closer until they coalesce, at which point the interval of coexistence shrinks to zero. The locus of points at which the surface in Fig. 6a folds back on itself is another manifestation of this phenomenon. To see this, it suffices to consider any one of the constant s_1^f contours of the surface. As s_2^f decreases along the contour, the two branches of the contour approach each other until they coalesce at a sufficiently small value of s_2^f.

Projection of the constant D contours of the surface in Fig. 6a onto the $s_1^f s_2^f$-plane yields the family of straight lines shown in Fig. 6b. To understand the significance of this family, consider any one member of the family corresponding to a given dilution rate. Then, at this dilution rate, C_2 cannot exist if the feed concentrations lie below the line; coexistence is feasible only if the feed concentrations lie above the line. We discuss below in Section 3.3.3 the reasons for the remarkably simple geometry of the constant D contours.

3.3.2. *The boundary between extinction of C_1 and coexistence*

A similar surface separating the region of coexistence from the region in which C_1 vanishes can also be found; it is determined by the conditions

$$r_1^g = D, \quad r_2^g = D, \quad c_1 = 0.$$

This surface turns out to have a fairly complex geometry: It folds three times for some range of feeds, and only once for others (Fig. 7a). Recall that for $s_1^f = 0.05$ g/l, $s_2^f = 2$ g/l there were two values for D_1^c. This is because the surface is triple-valued for this set of feed concentrations. The surface is also different because "inside" signifies the inability of C_1 to survive in the presence of C_2, while "outside" signifies the possibility of coexistence. In Section 3.3.1, we argued that the fold of the surface in Fig. 6a represents the locus of points at which D_2^w and D_2^c coalesce. In Fig. 7a also, the folds can be thought of as the locus of points at which two critical dilution rates coalesce.

Projection of the constant D contours of the surface onto the $s_1^f s_2^f$-plane also yields a family of straight lines (Fig. 7b). In this case, however, the significance is slightly different. Consider once again the straight line corresponding to a given dilution rate. Then, at this dilution rate, C_1 cannot exist if the feed concentrations are above the line; hence, coexistence is feasible only if the feed concentrations lie below the line.

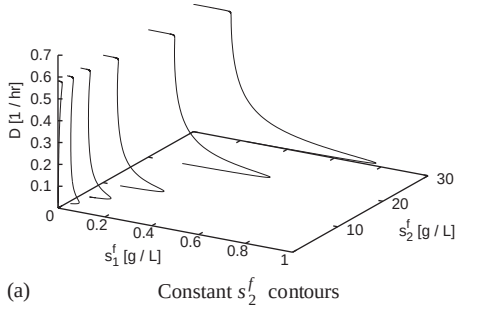

(a) Constant s_2^f contours

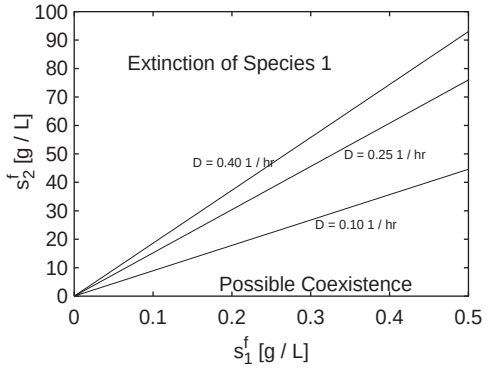

(b) Projection of constant D contours onto the $s_1^f s_2^f$-plane.

Fig. 7. Contours of the surface in the $s_1^f s_2^f D$-space separating the coexistence region from the region in which C_2 is outcompeted. (a) "Inside" the surface, C_1 vanishes; "outside" the surface, both species can coexist. (b) At each dilution rate, C_1 cannot exist at feed concentrations lying above the line corresponding to that dilution rate.

3.3.3. The operating diagram

Before constructing the operating diagram, it is useful to explain why the projections of the constant D contours in Figs. 6b and 7b are straight lines passing through the origin. This physical insight simplifies the construction of the operating diagram.

To understand the geometry of the constant D contours, observe that at a coexistence steady state, Eq. (5) implies that

$$r_{11}^s c_1 + r_{21}^s c_2 = D(s_1^f - s_1),$$

$$r_{12}^s c_1 + r_{22}^s c_2 = D(s_2^f - s_2).$$

Now, the specific uptake rates, r_{ij}^s, are functions of D, since coexistence steady states are completely determined by the dilution rate [see Eq. (B.10)]. Moreover, the substrate concentrations at a coexistence steady state are negligibly small compared to the feed concentrations at all but the highest dilution rates and the smallest feed concentrations. Under these conditions, coexistence steady states satisfy the vectorial relation

$$c_1 \mathbf{r}_1^s + c_2 \mathbf{r}_2^s = D\mathbf{s}^f, \quad \mathbf{r}_i^s \equiv \begin{bmatrix} r_{i1}^s \\ r_{i2}^s \end{bmatrix}, \quad \mathbf{s}^f \equiv \begin{bmatrix} s_1^f \\ s_2^f \end{bmatrix}.$$

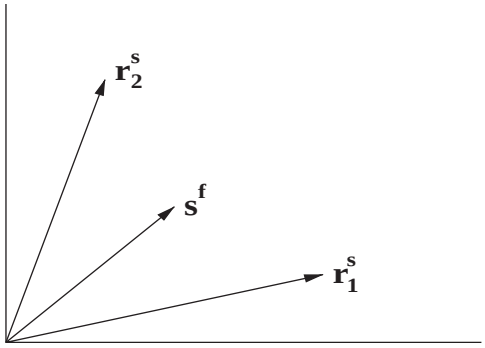

Fig. 8. The substrate consumption vectors, $\mathbf{r}_i^s(D)$, and the feed concentration vector, $\mathbf{s}^f$. There is coexistence if and only if $\mathbf{s}^f$ lies between the substrate consumption vectors. If $\mathbf{s}^f$ lies above $\mathbf{r}_2^s$, c_1 vanishes; if $\mathbf{s}^f$ lies below $\mathbf{r}_1^s$, c_2 vanishes.

It follows that a non-trivial steady state ($c_1, c_2 > 0$) exists if and only if the feed concentration vector, $\mathbf{s}^f$, lies between the substrate consumption vectors, $\mathbf{r}_1^s$ and $\mathbf{r}_2^s$ (Fig. 8). Moreover, C_1 vanishes if $\mathbf{s}^f$ coincides with or lies above the vector $\mathbf{r}_2^s$, and C_2 vanishes if $\mathbf{s}^f$ coincides with or lies below the vector $\mathbf{r}_1^s$. The constant D contours in Figs. 6b and 7b lie precisely along the vectors $\mathbf{r}_1^s$ and $\mathbf{r}_2^s$, respectively. As D changes, the substrate consumption vectors, $\mathbf{r}_i^s$, rotate. The fold points on the surface in Fig. 6b [Fig. 7b, resp.] occur when the consumption vector for C_1 (C_2, resp.) changes the direction of its rotation.

This suggests a concise method of depicting the operating diagram. Let $\theta_1(D)$ denote the angle made by the constant D contours in Fig. 7b with the s_1^f-axis, $\theta_2(D)$ denote the angle made by the constant D contours in Fig. 6b with the s_1^f-axis, and θ_s denote the angle made by the feed concentration vector with the s_1^f axis:

$$\theta_1(D) \equiv \arctan\left(\frac{r_{22}^s}{r_{21}^s}\right), \quad \theta_2(D) \equiv \arctan\left(\frac{r_{12}^s}{r_{11}^s}\right),$$

$$\theta_s \equiv \arctan\left(\frac{s_2^f}{s_1^f}\right).$$

Then, at any dilution rate small enough to ensure that $s_j \ll s_j^f$, coexistence is possible only if the feed concentrations are such that θ_s lies between θ_1 and θ_2. Fig. 9 shows the graphs of θ_1 and θ_2 as functions of the dilution rate. The non-trivial steady state exists if and only if θ_s lies between the two curves.

Fig. 9 shows that if the feed concentration of one of the substrates is held fixed and the feed concentration of the other substrate is raised progressively, we eventually reach a region where coexistence is impossible. To understand this result, we appeal to Phillips, who first noted the inevitability and ecological significance of this result (Phillips, 1973). Without loss of generality, take s_2^f to be fixed and raise s_1^f; then the point will eventually pass into the extinction region of C_2. This is because as

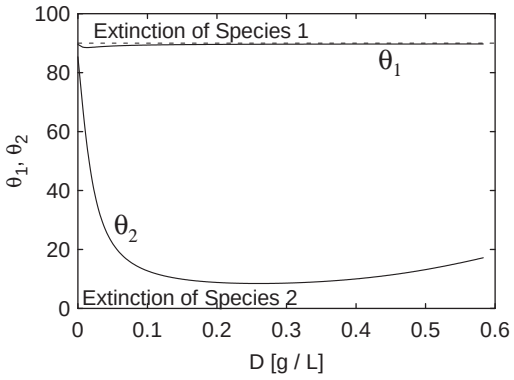

Fig. 9. The operating region for coexistence. At any given dilution rate, coexistence is feasible only if the feed concentrations are such that $\theta_s \equiv \arctan(s_2^f/s_1^f)$ lies between θ_1 and θ_2.

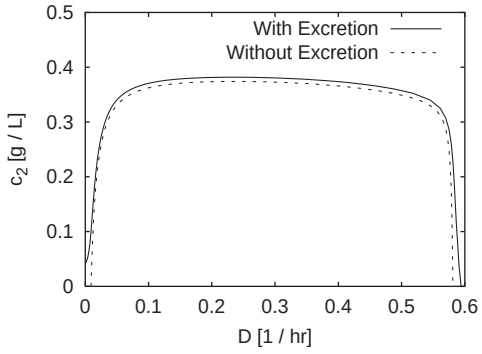

Fig. 10. Variation of c_2 with respect to D in the presence of excretion (solid) and in the absence (dashed). Note that with excretion c_2 does not vanish, no matter how small the dilution rate. This is in contrast to the previous results. The simulations in the presence of excretion were performed with $\alpha = 0.1$, $s_1^f = 1$ g/l, and $s_2^f = 2$ g/l.

s_1^f becomes large, so does the density of C_1. Consequently, no matter how high we choose the value for s_2^f, the density of C_1 will eventually become so high that it will consume a major part of S_2 even though S_2 is not its preferred substrate. Hence, C_2 will become extinct because it is overwhelmed by the high population density of C_1.

3.4. Influence of excretion on coexistence

To study the effect of excretion on coexistence of the two species, we modified the model as follows. We assumed that a certain fraction, α, of the specific growth rate of C_1 is diverted to production of an excretory product, say S_3, and C_2, but not C_1, can consume S_3 as a substrate. This introduces two additional mass balances that account for the evolution of S_3 and E_{23}

$$\frac{ds_3}{dt} = \alpha r_1^g c_1 - D s_3 - r_{23}^s c_2, \quad r_{23}^s \equiv V_{23}^s e_{23}\sigma_{23},$$

$$\frac{de_{23}}{dt} = r_{23}^e + r_{23}^* - r_{23}^d - r_2^g e_{23}, \quad r_{23}^e \equiv V_{23}^e \frac{e_{23}\sigma_{23}}{\bar{K}_{23}^e + e_{23}\sigma_{23}}$$

and the specific growth rate of C_2 becomes

$$r_2^g \equiv Y_{21} r_{21}^s + Y_{22} r_{22}^s + Y_{23} r_{23}^s.$$

All other equations and kinetics remain unchanged.

The numerical studies of this model with $\alpha = 0.1$ indicate that the coexistence space increases. Fig. 10 is a plot of $c_2|_{\phi_{A1}}$ vs. D at fixed feed concentrations, $s_1^f = 1$ g/l and $s_2^f = 2$ g/l, for both models (with and without excretion). Note that at most dilution rates, c_2 is increased almost insignificantly. However, the most stiking difference is c_2 does not drop to zero even at the smallest dilution rates.

To find the boundary between coexistence of both species and extinction of C_2, we seek, once again, the surface satisfying the conditions

$$r_1^g = D, \quad r_2^g = D, \quad c_2 = 0.$$

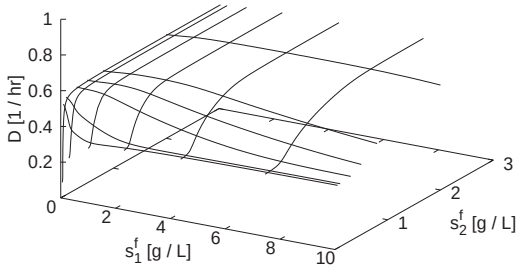

Fig. 11. Bounding surface for C_2 with acetate excretion, $\alpha = 0.1$. Species 2 may exist in the presence of Species 1 below this surface. Note that the surface is single-valued, in contrast to the same surface computed for the model without excretion (Fig. 6a).

This surface is plotted in Fig. 11 with the dilution rate on the vertical axis and the feed concentrations on the horizontal axes. The excretion parameter α is still set to 0.1. The surface is single-valued for most feed concentrations because there is now typically only one dilution rate at which c_2 becomes zero—the washout dilution rate, D_2^w. There is coexistence at *all* points below the surface. It follows that excretion by C_1 of a product that can be consumed by C_2 increases the region in which C_2 exists.

The disappearance of the competition dilution rate, D_2^c, in the presence of excretion is not surprising. We noted above that in the absence of excretion, C_2 vanished at low dilution rates only if s_1^f/s_2^f was sufficiently large, and that this occurred because under these conditions, the density of C_1 became much larger than the density of C_2. Now, if C_1 excretes a product, S_3, then a high density of C_1 implies significant production of S_3, a substrate that can be consumed by C_2 only. Hence, the very same conditions that in the absence of excretion led to washout of C_2 result in a large supply of S_3 in the presence of excretion; this can be consumed by C_2 without any competition from C_1. Existence of C_1, therefore, implies the existence of C_2.

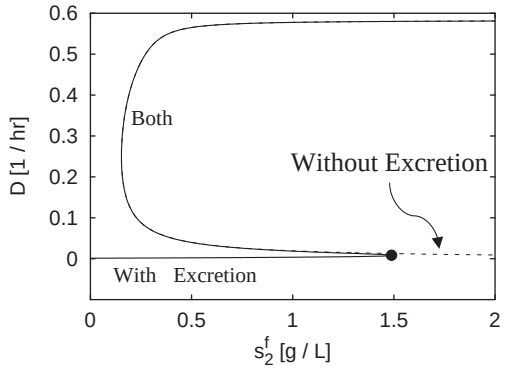

Fig. 12. A plot of a contour of the bounding surface for C_2 for s_1^f fixed at 1 g/l. The contour for the model without excretion (dashed) can also be found in Fig. 6a as the left-most curve. The solid curve is the contour for the model with excretion, $\alpha = 0.0016$. Note that the two are indistinguishable until the excretion curve folds near $s_2^f = 1.5$ g/l (solid circle). This extra fold means coexistence is possible in the limit of very low dilution rates.

The bounding surface for C_1 does not change, because setting $c_1 = 0$ implies $s_3 = 0$, so that the growth rate of C_2 reverts to the original definition of r_2^g. Thus, since the space for existence of C_2 increased, and the corresponding space for C_1 remained the same, the overall coexistence space increased.

The effect of varying the parameter α was also investigated. One would expect that if α is taken to be very close to zero, the surface for the extinction of C_2 would be qualitatively similar to that found in Fig. 6a. However, numerical studies show that this is not the case. That is, a plot of the points of extinction of C_2 at $s_1^f = 1$ g/l and $\alpha = 0.00016$ reveal coexistence in the limit as $D = 0$ (see Fig. 12).

4. Conclusions

We extended our earlier structured model for growth of a single species on two substitutable substrates to accommodate the growth of two species on two substitutable substrates. Our goal was to determine

1. The dilution rates and feed concentrations at which both species coexist.
2. The influence of excretion on this region of coexistence.

In the course of our studies, we found that:

1. If the interaction between the two species is purely competitive, the coexistence region is completely determined by the flow rate and the ratio of the feed concentrations. This suggests that the most fruitful method for acquiring the data is to hold the flow rate fixed and vary the ratio of the feed concentrations (see Fig. 9).
2. If the interaction between the two species is commensalistic, the coexistence region is significantly enhanced, since one of the species cannot vanish due to competition.

Acknowledgements

During the course of this research, Gregory Reeves was partially supported by the University Scholars Program at the University of Florida.

Appendix A. Derivation of the reduced equations (5)–(7)

We show here that for all but the smallest initial time intervals, Eqs. (1)–(4) can be approximated by the reduced equations (5)–(7). To see this, observe that:

1. In each species, the sum of the concentrations of all the intracellular components is unity. That is

$$(x_{i1} + e_{i1}) + (x_{i2} + e_{i2}) + c_i^- = 1 \text{ g/gdw}, \quad i = 1, 2.$$

Hence, adding Eqs. (2)–(4) yields

$$0 = \sum_{j=1}^{2} (r_{ij}^s - r_{ij}^x + Y_{ij} r_{ij}^x) - \left(D + \frac{1}{c_i} \frac{\mathrm{d}c_i}{\mathrm{d}t} \right), \quad i = 1, 2$$

which may be rewritten as

$$\frac{\mathrm{d}c_i}{\mathrm{d}t} = \left(\sum_{j=1}^{2} r_{ij}^s - r_{ij}^x + Y_{ij} r_{ij}^x \right) c_i - D c_i, \quad i = 1, 2. \tag{A.1}$$

It is convenient to replace Eq. (4) by (A.1).

2. The inducer concentrations rapidly achieve quasi-steady state

$$\frac{\mathrm{d}x_{ij}}{\mathrm{d}t} = 0 \;\Rightarrow\; r_{ij}^x \approx r_{ij}^s,$$

where the last two terms in Eq. (2) have been neglected since loss of X_i due to dilution by growth and efflux of cells from the reactor is negligibly small compared to consumption of X_i by catabolism. It follows from this relation that

$$\frac{\mathrm{d}c_i}{\mathrm{d}t} = (r_i^g - D) c_i, \quad r_i^g \equiv \sum_{j=1}^{2} Y_{ij} r_{ij}^s$$

and

$$x_{ij} = \frac{r_{ij}^s}{k_{ij}^x} = \frac{V_{ij}^s e_{ij} s_j / (K_{ij}^s + s_j)}{k_{ij}^x}. \tag{A.2}$$

Substituting Eq. (A.2) in Eq. (3) yields

$$\frac{de_{ij}}{dt} = V^e_{ij}\frac{e_{ij}\sigma_{ij}}{\bar{K}^e_{ij} + e_{ij}\sigma_{ij}} + k^*_{ij} - k^d_{ij}e_{ij} - r^g_i e_{ij},$$

$$\bar{K}^e_{ij} \equiv \frac{K^e_{ij}k^x_{ij}}{V^s_{ij}}, \quad \sigma_{ij} \equiv \frac{s_j}{K^s_{ij} + s_j}.$$

Thus, we arrive at the reduced eight-dimensional system

$$\frac{ds_j}{dt} = D(s^f_j - s_j) - r^s_{1j}c_1 - r^s_{2j}c_2,$$

$$\frac{de_{ij}}{dt} = V^e_{ij}\frac{e_{ij}\sigma_{ij}}{\bar{K}^e_{ij} + e_{ij}\sigma_{ij}} + k^*_{ij} - k^d_{ij}e_{ij} - r^g_i e_{ij},$$

$$\frac{dc_i}{dt} = (r^g_i - D)c_i.$$

Appendix B. Analysis

In this section, we analyze the existence and stability of the steady states.

B.1. The trivial steady state ϕ_{00}

The trivial steady state, ϕ_{00}, satisfies $c_1 = c_2 = 0$. It follows from Eq. (5) that $s_j = s^f_j$. This makes intuitive sense because in the absence of the biomass, there is no consumption of either substrate.

We show below that ϕ_{00} is completely and uniquely determined by the feed concentrations; therefore, it is independent of the dilution rate, and exists for all $D > 0$. This result follows from a more general proposition: If the substrate concentrations are held constant, then the enzyme levels and specific growth rates approach a unique steady state. The uniqueness of ϕ_{00} now follows by letting the substrate concentrations be the feed concentrations. The proof of the more general proposition follows in two steps.

1. If the substrate concentrations are fixed, the enzyme levels are decreasing functions of the specific growth rate.

   To see this, observe that at steady state, Eq. (6) may be written as

   $$V^e_{ij}\frac{e_{ij}\sigma_{ij}}{\bar{K}^e_{ij} + e_{ij}\sigma_{ij}} + k^*_{ij} = (r^g_i + k^d_{ij})e_{ij}. \tag{B.1}$$

   Since the substrate concentrations are fixed, it immediately follows that the enzyme levels are a decreasing function of the specific growth rate. This is shown graphically in Fig. 13a. The analytical proof follows by recasting Eq. (B.1) in the form

   $$r^g_i = V^e_{ij}\frac{\sigma_{ij}}{\bar{K}^e_{ij} + e_{ij}\sigma_{ij}} + \frac{k^*_{ij}}{e_{ij}} - k^d_{ij}. \tag{B.2}$$

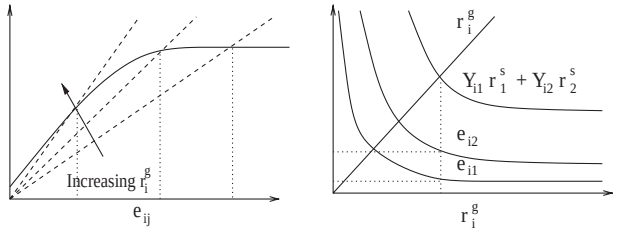

(a) At fixed s_1 and s_2, e_{ij} is a decreasing function of r^g_i.

(b) Uniqueness of r^g_i and e_{ij}.

Fig. 13. Steady-state enzyme levels at fixed substrate concentrations: (a) The full line shows the synthesis rate of E_{ij}; the dashed lines show the removal rate of E_{ij} at various specific growth rates. (b) Since e_{i1} and e_{i2} are decreasing function of r^g_i, so is $\sum_j Y_{ij}r^s_{ij}$; hence, Eq. (B.3) has a unique solution.

   Clearly, r^g_i is a decreasing function of e_{ij}; hence, e_{ij} is a decreasing function of r^g_i. We denote this function by $e_{ij}(r^g_i, s_j)$.

2. The steady-state specific growth rates and enzyme levels are uniquely determined by the substrate concentrations.

   This result follows directly from the definition of r^g_i

   $$r^g_i \equiv \sum_{j=1}^{2} Y_{ij}r^s_{ij} = \sum_{j=1}^{2} Y_{ij}V^s_{ij}e_{ij}(r^g_i, s_j)\sigma_{ij}. \tag{B.3}$$

   Now, the left-hand side of Eq. (B.3) increases with r^g_i, while the right-hand side decreases with r^g_i (Fig. 13b). Hence, there is a unique value of r^g_i satisfying Eq. (B.3). We conclude that the steady-state value of r^g_i is uniquely determined by s_1 and s_2. The uniqueness of the enzyme levels follows from the uniqueness of the specific growth rates.

We have shown above that the steady state is uniquely determined by the substrate concentrations. In particular, the trivial steady state, ϕ_{00}, is uniquely determined by the feed concentrations, and the specific growth rate of the ith species at this steady state, denoted $r^g_i|_{\phi_{00}}$, satisfies

$$r^g_i|_{\phi_{00}} \equiv \sum_{j=1}^{2} Y_{ij}r^s_{ij} = \sum_{j=1}^{2} Y_{ij}V^s_{ij}e_{ij}(r^g_i|_{\phi_{00}}, s^f_j)\sigma_{ij}(s^f_j). \tag{B.4}$$

In Appendix D (Section D.2), we show that ϕ_{00} is stable if and only if $D > r^g_1|_{\phi_{00}}$, $r^g_2|_{\phi_{00}}$. In other words, the stability of the trivial steady state depends on the ability of either species to survive at the feed concentrations. If $D > r^g_1|_{\phi_{00}}$, $r^g_2|_{\phi_{00}}$, then neither species can survive, and both species will be washed out of the reactor. If, on the contrary, $D < r^g_i|_{\phi_{00}}$, then C_i will persist in the reactor (assuming the absence of competition).

B.2. The semitrivial steady states ϕ_{10} and ϕ_{01}

Here, we show that the semitrivial steady state, ϕ_{10}, exists for all feed concentrations and for all sufficiently small dilution rates; furthermore, it is unique whenever it exists. The analysis of ϕ_{01} is analogous and is not presented here.

The steady state, ϕ_{10}, is characterized by the conditions, $r_1^g = D$ and $c_2 = 0$. The proof of its existence and uniqueness follows in two steps.

1. If the growth rate is fixed, the enzyme level, e_{1j}, is an increasing function of s_j.

   Substituting $r_1^g = a$ (a constant) into Eq. (B.1) with $i = 1$, we obtain

$$V_{1j}^e \frac{e_{1j}}{(\bar{K}_{1j}^e/\sigma_{1j}) + e_{1j}} + k_{1j}^* = (a + k_{1j}^d)e_{1j}. \tag{B.5}$$

   It follows immediately that e_{1j} is an increasing function of s_j. A graphical proof is shown in Fig. 14a. The analytical proof follows if we rewrite Eq. (B.5) in the form

$$\sigma_{1j} = \bar{K}_{1j}^e \frac{a + k_{1j}^d - k_{1j}^*/e_{1j}}{V_{1j}^e + k_{1j}^* - (a + k_{1j}^d)e_{1j}}. \tag{B.6}$$

   Then, σ_{1j} is an increasing function of e_{1j}. It follows that e_{1j} is an increasing function of σ_{1j}, and hence, of s_j.

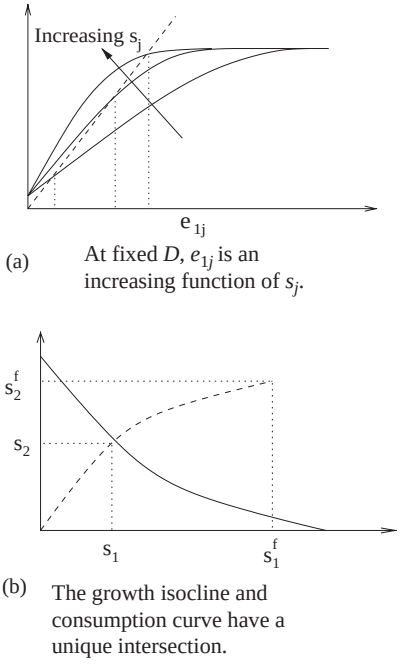

Fig. 14. Uniqueness of the semitrivial steady state ϕ_{10}: (a) The full lines show the synthesis rate of E_{1j} at various s_j; the dashed line shows the removal rate of E_{ij}. (b) The full line shows the growth isocline; the dashed line shows the consumption curve; the unique semitrivial steady state lies at the intersection of the two curves.

2. ϕ_{10} exists and is unique at all feed concentrations and sufficiently small dilution rates.

   First, we note that the condition, $r_1^g = D$, may be written as

$$\sum_{j=1}^{2} Y_{1j} V_{1j}^s e_{1j}(D, s_j)\sigma_{1j}(s_j) = D. \tag{B.7}$$

   This determines a curve on the s_1s_2-plane; Tilman calls it the *growth isocline* (Tilman, 1977). Since $e_{1j}(D, s_j)$ is an increasing function of s_j, the left-hand side of Eq. (B.7) is an increasing function of s_1 and s_2. It follows that the growth isocline is a graph of a decreasing function in the s_1s_2-plane (solid line in Fig. 14b). It can be shown that the larger the dilution rate, the further the distance from the origin of the corresponding growth isocline.

   Second, letting $c_2 = 0$ in Eq. (5) for both $j = 1, 2$, we obtain

$$\frac{(s_1^f - s_1)}{V_{11}^s e_{11}(r_i^g, s_1)\sigma_{11}} = \frac{(s_2^f - s_2)}{V_{12}^s e_{12}(r_i^g, s_2)\sigma_{12}}. \tag{B.8}$$

   This determines a curve on the s_1s_2-plane passing through the origin and the point (s_1^f, s_2^f); we shall call this the *consumption curve*. It can be shown that the left- and right-hand sides of Eq. (B.8) are decreasing functions of s_1 and s_2, respectively. Thus, the consumption curve is a graph of an increasing function in the s_1s_2-plane (Fig. 14b).

   Steady states occur at the points of intersection of the growth isocline and the consumption curve. Since the growth isocline decreases, and the consumption curve increases, there can be at most one steady state. There is exactly one steady state if the growth isocline lies on or below the growth isocline passing through (s_1^f, s_2^f); there is no steady state if the growth isocline lies above the growth isocline passing through (s_1^f, s_2^f). The dilution rate at which the growth isocline passes through (s_1^f, s_2^f) satisfies the equation

$$\sum_{j=1}^{2} Y_{1j} V_{1j}^s e_{1j}(D, s_j^f)\sigma_{1j}(s_j^f) = D. \tag{B.9}$$

   We denote this dilution rate by D_1^w, the washout dilution rate for C_1. We conclude that the steady state, ϕ_{10}, exists if and only if $D < D_1^w$; moreover, it is unique whenever it exists.

In Appendix D, Section D.3, we show that $r_2^g|_{\phi_{10}} \leqslant D$ is a necessary condition for stability of ϕ_{10}. This condition has a simple heuristic interpretation. The quantity, $r_2^g|_{\phi_{10}} - D$, is the overall specific growth rate of C_2 in the reactor where C_1 is resident. Consequently, if $r_2^g|_{\phi_{10}} - D > 0$, then once an arbitrarily small inoculum of C_2 is introduced into the reactor, it will successfully invade the reactor and either outcompete C_1 or coexist with C_1.

B.3. The non-trivial steady state ϕ_{11}

The non-trivial steady state ϕ_{11} satisfies the equations

$$r_i^g \equiv \sum_{j=1}^{2} Y_{ij} V_{ij}^s e_{ij}(D, s_j)\sigma_{ij} = D, \quad i = 1, 2. \tag{B.10}$$

It follows that ϕ_{11} exists only if Eq. (B.10) has a solution satisfying $0 < s_j < s_j^f$, $j = 1, 2$. Evidently, the enzyme and substrate concentration at the coexistence state are completely determined by the dilution rate.

Under what conditions does Eq. (B.10) have a solution? We show below that if both semitrivial steady states ϕ_{10} and ϕ_{01} exist, and one of the following holds

1. $r_1^g|_{\phi_{01}}$, $r_2^g|_{\phi_{10}} > D$,
2. $r_1^g|_{\phi_{01}}$, $r_2^g|_{\phi_{10}} < D$.

Then Eq. (B.10) admits a solution with $0 < s_j < s_j^f$, $j = 1, 2$. Both conditions (1) and (2) allow a simple heuristic explanation. Condition (1) states that either species can successfully invade a reactor inhabited by the other species. In this case, a stable coexistence steady state exists and is stable. Condition (2) states that neither species can invade a reactor inhabited by its competitor. In this case, an unstable coexistence steady state exists, but is unstable, so that a small perturbation in the environment would typically drive one species to extinction, while the other species would persist at the corresponding semitrivial steady state.

To prove this assertion, we observe that the functions r_i^g in Eq. (B.10) are strictly increasing in both arguments s_1 and s_2. If condition (1) holds, then one of the following must be true:

- either $s_1|_{\phi_{10}} > s_1|_{\phi_{01}}$ and $s_2|_{\phi_{10}} < s_2|_{\phi_{01}}$;
- or $s_1|_{\phi_{10}} < s_1|_{\phi_{01}}$ and $s_2|_{\phi_{10}} > s_2|_{\phi_{01}}$;

because the two remaining alternatives contradict condition (1). Now suppose that the first combination is the case (see Fig. 15). In the s_1s_2-plane, the curve $r_1^g = D$ is a graph of a decreasing function passing through the point ϕ_{10}. This curve cannot intersect the segment that lies to the right of ϕ_{01} because everywhere on that segment $r_1^g > D$. Thus the curve must intersect the segment directly below ϕ_{01}. A similar argument shows that the curve $r_2^g = D$ must intersect the segment that lies to the left of ϕ_{10}. Since the curves $r_1^g = D$ and $r_2^g = D$ are continuous, they must intersect somewhere inside the shown rectangle and any such point of intersection provides a solution of Eq. (B.10). The proof proceeds along the same lines for the second possible combination in (1) or if condition (2) holds. We conclude that (1) or (2) provide sufficient conditions for Eq. (B.10) to have a feasible solution.

The above argument does not rule out the possibility of multiple coexistence steady states because the curves in Fig. 15 may intersect more than once.

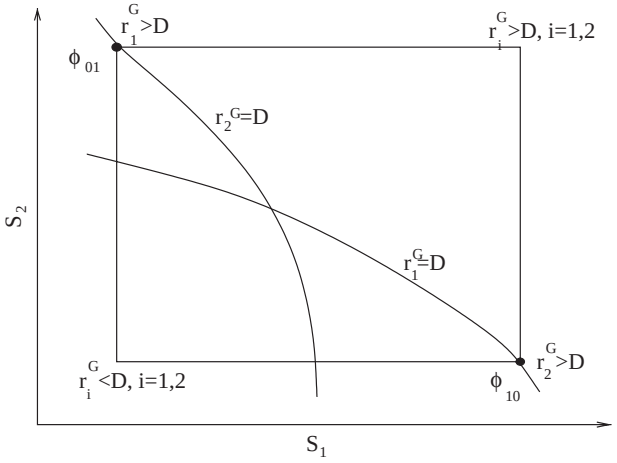

Fig. 15. Sufficient conditions for existence of the coexistence steady state ϕ_{11}.

Appendix C. Orders of magnitude of the parameters

For most substrates, the empirical values of V_{ij}^s, K_{ij}^s, V_{ij}^e, and $\bar{K}_{ij}^e$ are unknown. We show below that the orders of magnitude of the parameters can be estimated by requiring agreement with the following experimental observations:

1. The maximum enzyme level, e_{ij}^{max} is on the order of 1 mg/gdw (Ingraham et al., 1983).
2. The maximum specific substrate uptake rate is on the order of 1 g/gdw h (Andersen and Meyenburg, 1980).
3. The yield is on the order of 0.1–0.5 gdw/g (Andersen and Meyenburg, 1980).

It was assumed in the model that $\bar{K}_{ij}^e \sim e_{ij}^{max}$. Now according to the model:

1. The maximum enzyme level is on the order of $\sqrt{V_{ij}^e/(Y_{ij}V_{ij}^s)}$. Hence
$$\frac{V_{ij}^e}{V_{ij}^s} \sim 0.5(e_{ij}^{max})^2 = 0.5 \times 10^{-6}.$$
2. The maximum specific uptake rate is on the order of $V_{ij}^s e_{ij}^{max}$:
$$V_{ij}^s e_{ij}^{max} \sim 1 \text{ g/gdw h}.$$

It follows that $V_{ij}^s \sim 1000$ g/gdw h and $V_{ij}^e \sim 0.001$ g/gdw h.

Having determined the orders of magnitude, the parameter values of V_{ij}^e and $\bar{K}_{ij}^e$ were chosen in order

to obtain preassigned values of the maximum specific growth rates on each of the substrates.

Appendix D. Dynamics and stability

D.1. Dynamics of the enzymes

Here we analyze the dynamics of the enzymes of the ith species at fixed substrate concentrations; that is, we study the dynamics generated by the equations

$$\frac{de_{i1}}{dt} = V_{i1}^e \frac{e_{i1}\sigma_{i1}}{\bar{K}_{i1}^e + e_{i1}\sigma_{i1}} - \left(\sum_{j=1}^{2} Y_{ij} V_{ij}^s e_{ij}\sigma_{ij}\right) e_{i1} - k_{i1}^d e_{i1} + k_{i1}^*, \tag{D.1}$$

$$\frac{de_{i2}}{dt} = V_{i2}^e \frac{e_{i2}\sigma_{i2}}{\bar{K}_{i2}^e + e_{i2}\sigma_{i2}} - \left(\sum_{j=1}^{2} Y_{ij} V_{ij}^s e_{ij}\sigma_{ij}\right) e_{i2} - k_{i1}^d e_{i1} + k_{i1}^*, \tag{D.2}$$

at fixed s_1 and s_2. Solving for the nullclines in Eqs. (D.1) and (D.2), we obtain two functions

$$e_{i2} = W_1(e_{i1}) \equiv \frac{1}{Y_{i2} V_{i2}^s \sigma_{i2}} \left(V_{i1}^e \frac{\sigma_{i1}}{\bar{K}_{i1}^e + e_{i1}\sigma_{i1}} + \frac{k_{i1}^*}{e_{i1}} - Y_{i1} V_{i1}^s e_{i1}\sigma_{i1} - k_{i1}^d \right),$$

$$e_{i1} = W_2(e_{i2}) \equiv \frac{1}{Y_{i1} V_{i1}^s \sigma_{i1}} \left(V_{i2}^e \frac{\sigma_{i2}}{\bar{K}_{i2}^e + e_{i2}\sigma_{i2}} + \frac{k_{i2}^*}{e_{i2}} - Y_{i2} V_{i2}^s e_{i2}\sigma_{i2} - k_{i1}^d \right).$$

The functions $W_1(e_{i1})$ and $W_2(e_{i2})$ describe the e_{i1}- and e_{i2}-nullclines, respectively. We observe that

(a) both W_1 and W_2 are decreasing functions;

(b) $W_1 \to +\infty$ as $e_{i1} \to 0$ and $W_1 \to -\infty$ as $e_{i1} \to \infty$; similarly $W_2 \to +\infty$ as $e_{i2} \to 0$ and $W_2 \to -\infty$ as $e_{i2} \to \infty$;

(c) since s_1 and s_2 are fixed, Eqs. (D.1) and (D.2) admit a unique positive steady state, so that the graphs of W_1 and W_2 have only one point of intersection in the positive quadrant;

(d) $de_{i1}/dt < 0$ for $e_{i2} > W_1(e_{i1})$ and $de_{i1}/dt > 0$ for $e_{i2} < W_1(e_{i1})$; similarly $de_{i2}/dt < 0$ for $e_{i1} > W_2(e_{i2})$ and $de_{i2}dt > 0$ for $e_{i1} < W_1(e_{i2})$.

Observations (a)–(d) imply that the only possible phase diagram of Eqs. (D.1)–(D.2) is as shown in Fig. 16.

An important conclusion of the phase plane analysis is that the positive steady state of Eqs. (D.1)–(D.2) is locally asymptotically stable and the variational matrix

$$\frac{\partial(\dot{e}_{i1}, \dot{e}_{i2})}{\partial(e_{i1}, e_{i2})}$$

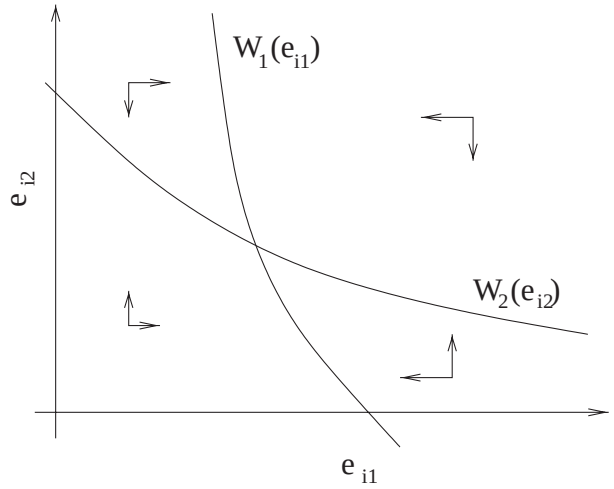

Fig. 16. Phase portrait of Eqs. (D.1)–(D.2). The curves labeled $W_1(e_{i1})$ and $W_2(e_{i2})$ represent the nullclines for e_{i1} and e_{i2}, respectively. The nullclines partition the $e_{i1}e_{i2}$-quadrant into four regions; the arrows show the orientation of the vector field in these four regions.

of Eqs. (D.1)–(D.2) at this steady state has two real negative eigenvalues. The eigenvalues must be real because the solutions near the steady state are not oscillatory.

D.2. Stability of ϕ_{00}

The variational matrix of Eqs. (5)–(7) at ϕ_{00} is given by

$$\begin{pmatrix} - & 0 & 0 & 0 & 0 & 0 & - & - \\ 0 & - & 0 & 0 & 0 & 0 & - & - \\ * & - & \frac{\partial(\dot{e}_{11},\dot{e}_{12})}{\partial(e_{11},e_{12})} & & 0 & 0 & 0 & 0 \\ - & * & & & 0 & 0 & 0 & 0 \\ * & - & 0 & 0 & \frac{\partial(\dot{e}_{21},\dot{e}_{22})}{\partial(e_{21},e_{22})} & & 0 & 0 \\ - & * & 0 & 0 & & & 0 & 0 \\ 0 & 0 & 0 & 0 & 0 & 0 & r_1^g - D & 0 \\ 0 & 0 & 0 & 0 & 0 & 0 & 0 & r_2^g - D \end{pmatrix}.$$

Here we denote all positive entries by $+$, all negative entries by $-$, and by $*$ if the sign is undetermined. The two blocks

$$\frac{\partial(\dot{e}_{11}, \dot{e}_{12})}{\partial(e_{11}, e_{12})} \quad \text{and} \quad \frac{\partial(\dot{e}_{21}, \dot{e}_{22})}{\partial(e_{21}, e_{22})}$$

contribute two negative eigenvalues each. Therefore, the first six eigenvalues of $J(\phi_{00})$ are strictly negative while the last two are given by $\lambda_7 = r_1^g|_{\phi_{00}} - D$ and $\lambda_8 = r_2^g|_{\phi_{00}} - D$. Thus, ϕ_{00} is stable if and only if $r_1^g|_{\phi_{00}} < D$ and $r_2^g|_{\phi_{00}} < D$.

D.3. Stability of ϕ_{10} and ϕ_{01}

The variational matrix of Eqs. (5)–(7) at ϕ_{10} is given by

$$\begin{pmatrix} - & 0 & - & 0 & 0 & 0 & - & - \\ 0 & - & 0 & - & 0 & 0 & - & - \\ * & - & \dfrac{\partial(\dot{e}_{11},\dot{e}_{12})}{\partial(e_{11},e_{12})} & & 0 & 0 & 0 & 0 \\ - & * & & & 0 & 0 & 0 & 0 \\ * & - & 0 & 0 & \dfrac{\partial(\dot{e}_{21},\dot{e}_{22})}{\partial(e_{21},e_{22})} & & 0 & 0 \\ - & * & 0 & 0 & & & 0 & 0 \\ + & + & + & + & 0 & 0 & 0 & 0 \\ 0 & 0 & 0 & 0 & 0 & 0 & 0 & r_2^g - D \end{pmatrix}.$$

The last eigenvalue of $J(\phi_{10})$ is given by $\lambda_8 = r_2^g|_{\phi_{10}} - D$. Therefore, the *sufficient* condition for instability of ϕ_{10} is given by the inequality $r_2^g|_{\phi_{10}} - D > 0$. We conjecture that this also a necessary condition for instability.

Stability analysis of $J(\phi_{01})$ is performed similarly.

References

Andersen, B., von Meyenburg, K., 1980. Are growth rates of bacteria in batch cultures limited by respiration? J. Bacteriol. 144, 114–123.

Aris, R., Humphrey, A.E., 1977. Dynamics of a chemostat in which two organisms compete for a common substrate. Biotechnol. Bioeng. 19, 1375–1386.

Chian, S.K., Mateles, R.I., 1968. Growth of mixed cultures on mixed substrates. Appl. Microbiol. 16, 1337–1342.

Egli, T., 1995. The ecological and physiological significance of the growth of heterotrophic microorganisms with mixtures of substrates. Adv. Microbiol. Ecol. 14, 305–386.

Fredrickson, A.G., Stephanopoulos, G., 1981. Microbial competition. Science 213, 972–979.

Fredrickson, A.G., 1977. Behavior of mixed cultures of microorganisms. Ann. Rev. Microbiol. 31, 63–87.

Fredrickson, A.G., Tsuchiya, H.M., 1977. Microbial kinetics and dynamics. In: Lapidus, L., Amundson, N.R. (Eds.), Chemical Reactor Theory: A Review. Prentice-Hall, Englewood Cliffs, NJ, pp. 405–483 (Chapter 7).

Gottschal, J.C., 1986. Mixed substrate utilization by mixed cultures. In: Poindexter, J.S., Leadbetter, E.R. (Eds.), Bacteria in Nature. Plenum Press, New York, pp. 261–292.

Gottschal, J.C., 1993. Growth kinetics and competition—some contemporaneous comments. Antonie van Leeuwenhoek 63, 299–313.

Hansen, S.R., Hubbell, S.P., 1980. Single nutrient microbial competition: agreement between experimental and theoretical forecast outcomes. Science 207, 1491–1493.

Harder, W., Dijkhuizen, L., 1976. Mixed substrate utilization. In: Dean, A.C.R., Ellwood, D.C., Evans, C.G.T., Melling, J. (Eds.), Continuous Culture 6: Applications and New Fields. Ellis Horwood, Chichester, pp. 297–314 (Chapter 23).

Harder, W., Dijkhuizen, L., 1982. Strategies of mixed substrate utilization in microorganisms. Philos. Trans. R. Soc. London B 297, 459–480.

Harrison, D.E.F., Wren, S.J., 1976. Mixed microbial cultures as a basis for future fermentation processes. Process Biochem. 11, 30–32.

Hutchinson, G.E., 1961. The paradox of the plankton. Am. Nat. 95, 137–145.

Ingraham, J.L., Neidhardt, F.C., Maalœ, O., 1983. Growth of the Bacterial Cell. Frank Sinauer Associates, Sunderland, MA.

Ingram, L.O., Aldrich, H.C., Borges, A.C.C., Causey, T.B., Martinez, A., Morales, F., Saleh, A., Underwood, S.A., Yomano, L.P., York, S.W., et al., 1999. Enteric bacterial catalysts for fuel ethanol production. Biotechnol. Prog. 15, 855–866.

Kim, S.U., Dhurjati, P., 1986. Analysis of two interacting bacterial populations with opposite substrate preferences. Biotechnol. Bioeng. 29, 1015–1023.

Kuznetsov, Y.A., 1998. CONTENT—Integrated environment for analysis of dynamical systems.

León, J.A., Tumpson, D.B., 1975. Competition between two species for two complementary or substitutable resources. J. Theor. Biol. 50, 185–201.

Muller, S., Losche, A., Mertingk, H., Beisker, W., Babel, W., 2000. Flow cytometric monitoring of *Rhodococcus erythropolis* and *Ochrobactrum anthropi* in a mixed culture. Acta Biotechnol. 20, 219–233.

Narang, A., 1998a. The steady states of microbial growth on mixtures of substitutable substrates in a chemostat. J. Theor. Biol. 190, 241–261.

Narang, A., 1998b. The dynamical analogy between microbial growth on mixtures of substrates and population growth of competing species. Biotechnol. Bioeng. 59, 116–121.

Narang, A., Konopka, A., Ramkrishna, D., 1997. The dynamics of microbial growth on mixtures of substrates in batch reactors. J. Theor. Biol. 184, 301–317.

Pavlou, S., Fredrickson, A.G., 1989. Growth of microbial populations in nonminimal media: some considerations for modeling. Biotechnol. Bioeng. 34, 971–980.

Phillips, O.M., 1973. The equilibrium and stability of simple marine biological systems. I. Primary nutrient consumers. Am. Nat. 107, 73–93.

Porter, J., Pickup, R.W., 2000. Nucleic acid-based fluorescent probes in microbial ecology: application of flow cytometry. J. Microbiol. Meth. 42, 75–79.

Powell, E.O., 1958. Criteria for the growth of contaminants and mutants in continuous culture. J. Gen. Microbiol. 18, 259–268.

Rogers, J.B., DuTeau, N.M., Reardon, K.R., 2000. Use of 16S-RNA to investigate microbial population dynamics during biodegradation of toluence and phenol by a binary culture. Biotechnol. Bioeng. 70, 436–445.

Tilman, D., 1977. Resource competition between planktonic algae: an experimental and theoretical approach. Ecology 58, 338–348.

Wolfram, S., 1999. The Mathematica book, 4th Edition. Wolfram-Media, Champaign, IL.